# Further Studies of Anomalous Inelastic Proton Scattering

BERNARD L. COHEN AND ALLEN G. RUBIN
*Oak Ridge National Laboratory,* Oak Ridge, Tennessee*
(Received May 12, 1958)

Anomalous inelastic proton scattering was studied by (1) determining its dependence on bombarding energy, (2) measuring the energy distributions with greatly improved energy resolution, (3) extending the data to separated isotopes and to elements not previously investigated because of target preparation difficulties, and (4) observing the energy distribution of the de-excitation gamma rays following the reaction. In (1), the anomalous peak is found to stay at the same $Q$ value as the bombarding energy is varied. This indicates that the effect is not due to a giant resonance effect but rather, to the regular occurrence of a certain type of level in the final nucleus. In (2), many low-lying levels are resolved; a strong correlation is found between their cross sections for excitation in these reactions and in Coulomb excitation, and an anticorrelation is found between their cross sections for excitation in these reactions and in $(p,d)$ reactions. This is interpreted as good evidence that the reactions used here strongly excite collective levels and only weakly excite single-particle transitions. The fine structures of the anomalous peaks differ greatly among neighboring nuclides reflecting even-*versus*-odd and closed-shell effects; however, the gross structure as obtained with poor resolution is very similar for neighboring elements. A few striking similarities between the spectra of several elements are pointed out. Several levels of known spin and parity are identified as contributing strongly to the anomalous peak. In (3), it is found that anomalous inelastic scattering ends by becoming irregular and weak between atomic numbers 54 and 64; it is apparently present in every isotope of every element between atomic numbers 30 and 53. In (4), gamma-ray transitions direct to the ground state following anomalous inelastic scattering are found to be relatively common.

Many theoretical explanations for anomalous inelastic scattering are excluded by these results; there is reasonably good evidence that it arises from some type of collective excitation "dissolved" among many shell model states in that energy region.

## INTRODUCTION

IT has previously been shown[1,2] that the energy distributions of protons emitted from inelastic scattering of 23-Mev protons by various medium weight and heavy nuclei are characterized by strong peaks at energies about 2.5 Mev below the maximum energy. Moreover, there are strong regularities in these peaks among neighboring elements in the periodic table as regards the energy at which they occur, the cross section for their excitation, and their angular distributions. These regularities extend to elements of both even and odd atomic number, and even across closed shells. Since this effect was most unexpected from usual theories, it has been referred to as "anomalous" inelastic scattering.[1]

In this paper, we present the results of investigations of several other aspects of this phenomenon. These include (1) the dependence of the effect on bombarding energy, (2) the fine structure of the anomalous peak as obtained with greatly improved energy resolution, (3) the extension of these studies to regions of the periodic table not previously investigated, and (4) a preliminary investigation of the energy spectrum of the de-excitation gamma rays following anomalous inelastic scattering. In the course of (2), measurements were also made on some of the lower lying states excited by inelastic proton scattering, and an interesting correlation between this process and Coulomb excitation was observed. As a result of all these studies and further consideration of some of the previous data, tentative conclusions are reached on the theoretical explanation for anomalous inelastic scattering.

* Operated for the U. S. Atomic Energy Commission by Union Carbide Corporation.
[1] B. L. Cohen, Phys. Rev. **105**, 1549 (1957).
[2] B. L. Cohen and S. W. Mosko, Phys. Rev. **106**, 995 (1957).

## EXPERIMENTAL

### 1. Dependence on Bombarding Energy

The experimental arrangement for studying the dependence of anomalous inelastic scattering on incident proton energy is shown schematically in Fig. 1. The energy is varied by passing the incident beam through an aluminum absorber about two inches in front of the target. This introduces the following complications:

(a) The beam is multiply scattered so that an appreciable fraction of it strikes the target holder which then can scatter it into the detector.

(b) The multiple scattering causes an appreciable part of the beam to miss the Faraday cup.

(c) The absorber acts as a strong source of scattered protons and of gamma rays.

To circumvent (a), a collimating system, consisting of collimators $A$ and $C$, is used to prevent protons originating at the target holder from reaching the detector. Effect (b) is reduced by extending the Faraday cup close to the target. The residual effect is corrected for by measuring the Faraday-cup currents with ab-

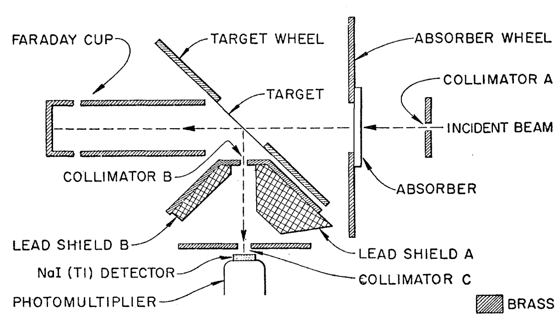


FIG. 1. Experimental arrangement for varying bombarding energy. Operation is explained in text.

sorbers alternately in and out of the beam without changing cyclotron operating conditions. The largest correction needed was 30%. Effect (c) was sufficiently reduced by inserting a shield, ($A$), between the absorber and detector.

## 2. Improved Energy Resolution Studies

The previous work[1,2] was carried out with essentially the best energy resolution obtainable with scintillation spectroscopy techniques. In order to improve the resolution, it was therefore necessary to use magnetic analysis. The magnet for analyzing the scattered particles was originally designed to bend energetic fission fragments 40 degrees with a focal length of about five feet.[3] Such a long focal length was unacceptable for the present application both because of space limitations and because of the great intensity loss resulting from the small solid angle of acceptance it implies. The magnet was, therefore, converted to bend 60 degrees with single focusing by attaching 10-degree wedges to each end of each poleface. The combined thickness of these wedges was twice the magnetic gap, and their mean width was half of the latter. While this situation is far from ideal, magnetic measurements indicated that the magnetic field follows the geometry of the modified polefaces reasonably well in the regions of the particle trajectories. Due to saturation effects, however, the magnetic field in the region of the wedges does not change proportionally to the magnetic field in the central region as the magnet current is changed. This introduces a very serious complication into the determination of energies, which in conventional magnetic analyzing systems are simply proportional to the square of the measured magnetic fields. Energy measurements, therefore, had to be made by applying a correction to the value determined from magnetic measurements, this correction being obtained from $Q$ values of known levels. This procedure is relatively unsatisfactory, and there was also some evidence that the factors necessitating it were not completely reproducible, so that the $Q$ values obtained in this work may be in error by as much as 150 kev.

The energy spread of the incident proton beam was limited by a magnetic analyzing system based on a 15-degree magnet; the object for the system was a $\frac{1}{8}$-in. wide by $\frac{3}{4}$-in. high slit near the cyclotron, and the image in most cases was the target itself, cut into a narrow strip. The current was monitored by a scintillation counter detecting elastically scattered protons from the target. In some of the later work, wide targets were used; the image of the beam analyzing system was then a slit placed 5 in. in front of the target, and the current was monitored with a Faraday cup.

The scattered particles, after passing through the 60-degree magnet, were detected simultaneously at six positions on the focal plane of that system, each detector representing an adjacent energy interval. The

[3] Cohen, Cohen, and Coley, Phys. Rev. **104**, 1046 (1956).

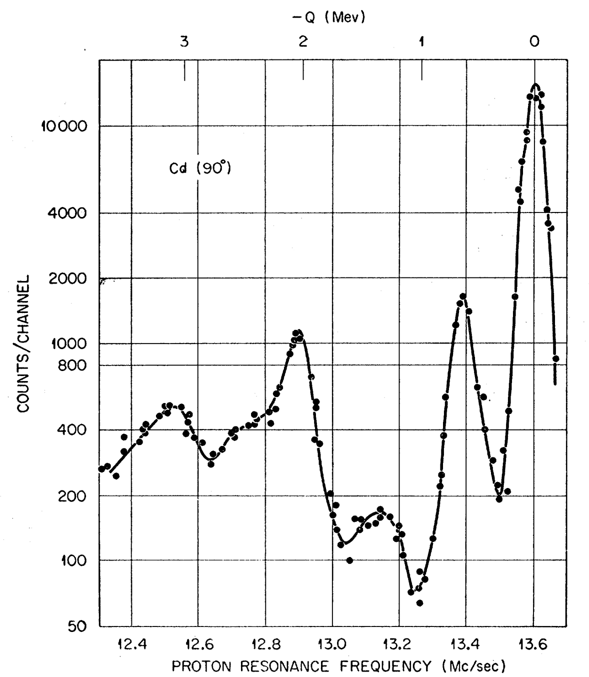


FIG. 2. Energy distribution of protons inelastically scattered from cadmium as measured with magnetic analyzing system. The magnetic field is proportional to the proton resonance frequency.

detectors were CsI(Tl) crystals $\frac{1}{4}$-in. wide by $\frac{1}{8}$-in. thick by 2-in. high; the pulses from each were processed by separate photomultiplier-amplifier-scaler systems. An absorber in front of the detectors eliminated alpha particles and reduced deuteron energies to considerably less than half of the proton energy. The amplifier discrimination levels were set at about half of the proton pulse height, so that pulses from deuterons and most gamma rays were rejected. The residual gamma-ray background was virtually eliminated by lead shielding around the detectors.

The energy resolution of this type of system is determined principally by the widths of the objects and images of the two magnetic analyzing systems, and the target thickness. All of these were set to give approximately equal contributions to the resolution, with total resolution of about 180 kev full width at half-maximum. As a test for imperfections in the ion optics, all of these factors were reduced by a factor of four; the resolution achieved was about 80 kev, indicating that such imperfections did not contribute more than 65 kev to the resolution spread. This is probably the limitation introduced by the conversion of the magnet with wedges.

Each detector covered a 125-kev energy interval, so that with the six detectors, a 750-kev interval was measured simultaneously. Magnet settings were made approximately 500 kev apart so that there was a considerable overlap in measurements with adjacent settings. The magnetic field was measured with a nuclear fluxmeter employing proton resonance. A typical measurement is shown in Fig. 2.

### 3. Extension to Previously Unstudied Elements

In the previous work, essentially all measurements were made with targets of thin metal foils. This limitation did not allow measurements for elements between $_{52}$Te and $_{78}$Pt (with the single exception of $_{73}$Ta), or between $_{30}$Zn and $_{40}$Zr (with the exception of $_{34}$Se), in spite of the fact that there were strong indications that these regions would be very interesting. The simplest general method for making thin targets of these elements is by preparing a suspension in polystyrene of fine powders of chemical compounds containing them.[4] (In almost every case, the most suitable compound is the oxide.) This method introduces large quantities of carbon and oxygen into the target, and at 90 degrees, elastically scattered protons from these elements have an energy approximately equal to that of the anomalous inelastic peak in heavy elements.

The energy of the protons scattered from carbon and oxygen can be increased or decreased by observing at smaller or larger angles, respectively, but due to their very high relative intensity, it was not possible to achieve a clear-cut separation of these from the anomalous peak with scintillator resolution. It was therefore necessary to make these measurements by magnetic analysis. A detection angle of 45 degrees was used. Since target thicknesses were nonuniform, very thin targets ($\sim$7 mg/cm$^2$) were used, and even these contained only a relatively small fraction of the element being studied. In general, therefore, the statistical accuracy in these measurements was somewhat poorer than in the work with metal targets at 90 degrees. A few measurements were also made with metal targets at 45 degrees to serve as a comparison, since the intensity of the anomalous peak relative to the rest of the spectrum is lower at 45 degrees than at 90 degrees.[1]

### 4. Energy Spectrum of De-Excitation Gamma Rays

The energy spectrum of the de-excitation gamma rays following anomalous inelastic scattering was measured with a standard fast-slow coincidence arrangement. The protons were detected with a NaI(Tl) scintillation crystal 1 in. in diameter and $\frac{1}{8}$ in. thick. The amplifier produces a sharp marker pulse for the fast coincidence and amplifies the photomultiplier pulse. The latter is then fed to a single-channel analyzer which selects the anomalous group, and the output from the single-channel analyzer operates one-half of the slow coincidence circuit. The gamma rays were detected by a 3-in. by 3-in. NaI(Tl) scintillation crystal. The amplifier produces a sharp marker pulse for the other half of the fast coincidence, and the amplified photomultiplier pulse is fed to a 20-channel pulse-height analyzer. The latter is gated by a slow coincidence between the previously described fast coincidence and the output pulse from the single-channel analyzer. Thus, the 20-channel analyzer records the height of pulses in the gamma-ray detector which are in fast coincidence with protons from the anomalous peak. The resolving times were 0.1 and 2 microseconds for the fast and slow coincidence circuits, respectively.

The limiting factor on the rate of data accumulation is the total counting rate in the gamma-ray detector. To reduce gamma-ray background, the beam collimator was placed about five feet ahead of the target, and the beam was allowed to pass about five feet beyond the target before being stopped. Targets were made as thick as possible. A large amount of lead shielding was used around the gamma-ray detector, and a $\frac{3}{8}$-in. lead absorber was interposed between it and the target, since this preferentially absorbs low-energy gamma rays which are in greatest abundance. With all of these precautions, meaningful statistics could be obtained on the 20-channel analyzer in approximately one hour.

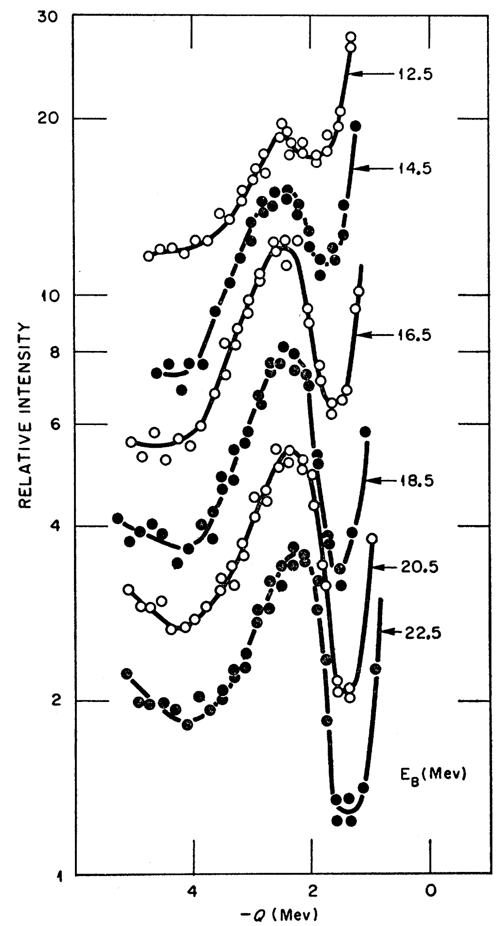


FIG. 3. Energy distribution of protons inelastically scattered by silver for various bombarding energies ($E_b$). Data for Zr, Cd, In, Sn, and CsI are very similar to this.

[4] N. S. Wall, Rev. Sci. Instr. 24, 1146 (1953).

The detecting crystals were about $1\frac{1}{4}$ in. from the center of the target; they were located at 90 degrees to the beam on opposite sides of it. Elastically scattered protons detected by the proton detector served as the current monitor.

## RESULTS AND CONCLUSIONS

### 1. Dependence on Bombarding Energy

Portions of the energy distributions of inelastically scattered protons from silver are shown in Fig. 3. In each case, the abscissa is the negative $Q$ of the reaction, i.e., the difference in energy from the incident proton in the center-of-mass system. The curves for silver are quite typical of those for all elements between atomic numbers 40 and 53 with the single exception of $_{41}$Nb for which no dip, or even point of inflection, was obtained to the right of the anomalous peak with 12.5-Mev bombarding energy. The lessening of this dip in silver (and other elements) with decreasing bombarding energy is explainable as deterioration of the energy resolution, plus the fact that the elastic peak becomes more intense.

The basic conclusion from these results is that anomalous inelastic scattering is not due to a giant resonance effect[5]—i.e., a standing wave for the outgoing proton in the nuclear potential. Such a standing wave would occur at a fixed energy of the outgoing proton rather than at a fixed value of $Q$, as is observed in Fig. 3. It thus appears that the phenomenon is essentially a nuclear structure effect arising from a regular occurence of certain types of nuclear energy levels, rather than a nuclear reaction effect arising from the nuclear potential.

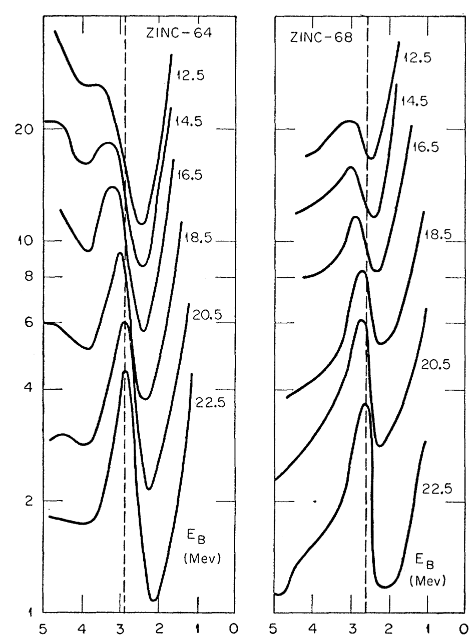


FIG. 4. Energy distribution of protons inelastically scattered by $Zn^{64}$ and $Zn^{68}$ for various bombarding energies ($E_b$).

[5] Feshbach, Porter, and Weisskopf, Phys. Rev. **96**, 448 (1954).

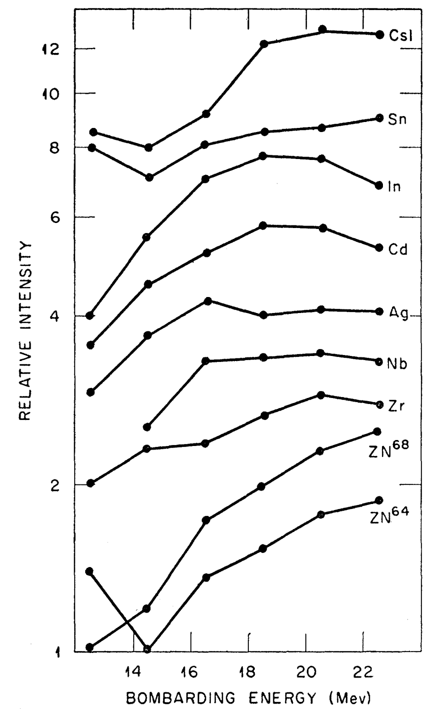


FIG. 5. Excitation function for anomalous inelastic scattering at 90 degrees in various elements.

Measurements similar to those of Fig. 3 were also made with a zinc target, and it was found that for that element the $Q$ value actually does shift slightly as the bombarding energy is changed. At about this time, isotopic targets of $Zn^{64}$ and $Zn^{68}$ were obtained, so that the measurements were repeated with each of these separately. The results are shown in Fig. 4. It is seen that the $Q$ value shifts to higher energies for each isotope independently as the bombarding energy is decreased. The shift is about 0.7 Mev over the range. For the elements between atomic numbers 40 and 55, the shift was determined to be $0.1\pm0.1$ Mev (in the same direction as for Zn), which is consistent with zero shift and certainly inconsistent with a shift comparable to that in the zinc isotopes.

The explanation for the large shifts in zinc is not clear. It is, of course, in the wrong direction and still more than an order of magnitude too small to explain the effect as a giant resonance. It may be that the mechanism for the reaction is changing, so that factors which favor other levels to be excited are coming into predominance. It does seem surprising, though, that the shifts should be identical in the two isotopes.

The dependence of the intensity of the anomalous group on bombarding energy is shown in Fig. 5. It is apparent that the effect varies slowly with bombarding

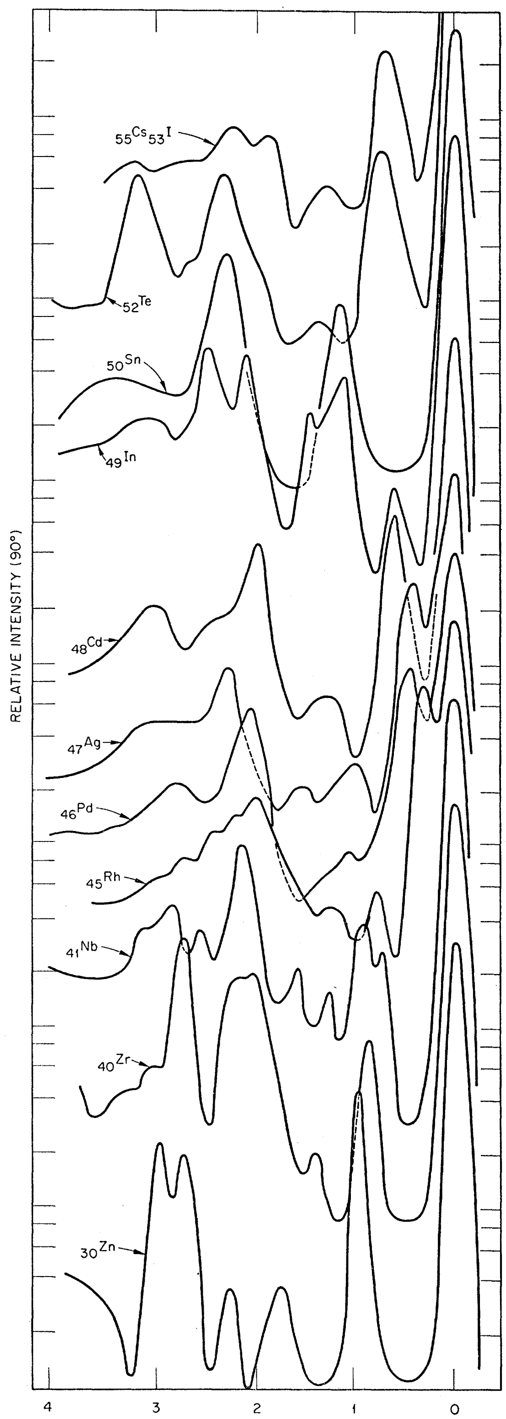


FIG. 6. Energy distribution of protons inelastically scattered from various elements (atomic numbers 40–55 and zinc) as measured with magnetic analysis. Observation angle was 90 degrees.

energy above about 15 Mev. For lower bombarding energies, the yield decreases rapidly with decreasing bombarding energies.

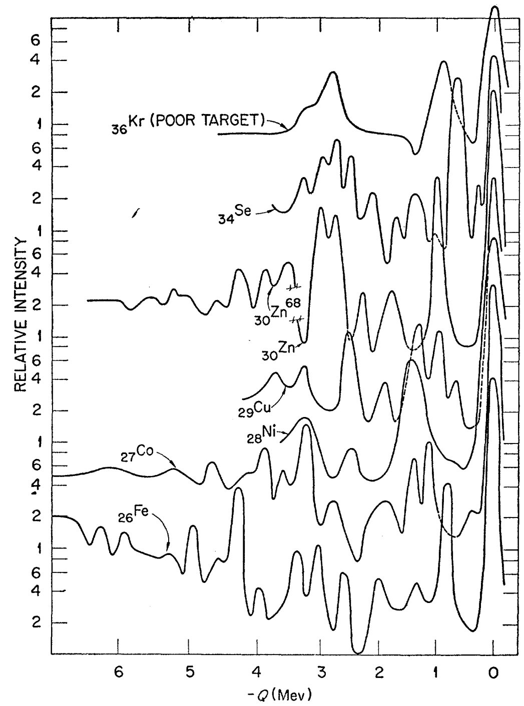


FIG. 7. Energy distribution of protons inelastically scattered from various elements (atomic numbers 26–36) as measured with magnetic analysis. Observation angle was 90 degrees.

## Improved Energy Resolution Studies

The energy distributions measured with magnetic analysis at 90 degrees are shown in Figs. 6, 7, and 8 for the three regions of the periodic table that were studied. From Fig. 6 it is clear that the peak in the $Z=40$ to 53 region is actually made up of a large number of groups. In general, there is little similarity among neighboring elements in this fine structure; the similarities are only apparent in the gross structure as measured with poor resolution. The fine structure exhibits the expected sparsity of levels near closed shells (e.g., Zr and Sn) and the expected higher level density in odd-even than in even-even elements, but there is no evidence for these effects in the gross structure. The same conclusion may be drawn from the Zn, Se, and Kr data of Fig. 7 and from the Pt and Au data of Fig. 8. In the Pb isotopes and Bi, most of the peaks do seem to be due to individual levels.

It is also instructive to note the very sharp structure observed for all elements in Fig. 7. These elements have recently been investigated with very high resolution by Buechner *et al.*[6]; in cobalt, between 2.0 and 3.6 Mev, 33 separate levels were found; and in the parts of that energy interval that they studied in copper, about 50 separate levels were found. In Fig. 7 each of these regions contains only three sharp peaks, one of which, in each case, rises in intensity by an order of magnitude

[6] W. W. Buechner *et al.*, Phys. Rev. **107**, 365 (1957); **108**, 373 (1957).

in less than 0.2 Mev. It is also interesting to note the very high $Q$ values to which the sharp structure extends. This is also noteworthy in the cases of Pt and Au shown in Fig. 8; these elements are expected to have very high level densities at these excitation energies. A similar comment might be made about the peak in Ta at $-Q=1.4$ Mev.

Another very interesting feature of the data in Figs. 6–8 is that the low-lying levels are also resolved, including, in most cases, the first excited states. These states have been investigated in great detail by Coulomb excitation[7]; in those investigations, the most important quantity extracted from the data is the reduced transition probability, $B(E2)$, measured in units of the single-particle value, $B(E2)_{SP}$. The correlation between this quantity and the cross section for excitation of these levels obtained from the data of Figs. 6–8 is shown in Fig. 9. It is quite clear that a strong correlation exists, i.e., levels that are excited strongly in Coulomb excitation are also strongly excited in inelastic proton scattering, and vice versa. In the case of Coulomb excitation, large values of $B(E2)$ may be straightforwardly interpreted as evidence that the levels are of a collective nature. The strong correlation in Fig. 9, therefore, indicates that collective levels are strongly excited in inelastic proton scattering, as has been predicted theoretically,[8] and that levels that are not of a collective nature are excited only weakly. Since the anomalous peaks are strongly excited in inelastic proton scattering, this indicates that they are probably due to some type of collective motion.

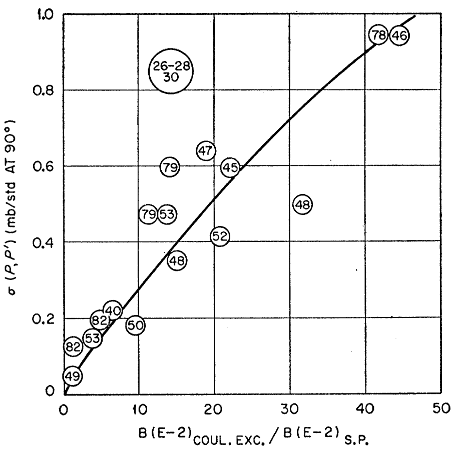


FIG. 9. Correlation between cross sections for exciting given levels by inelastic scattering of 23-Mev protons (ordinate) and Coulomb excitation [expressed as $B(E2)$-abscissa]. Figures are atomic numbers of elements.

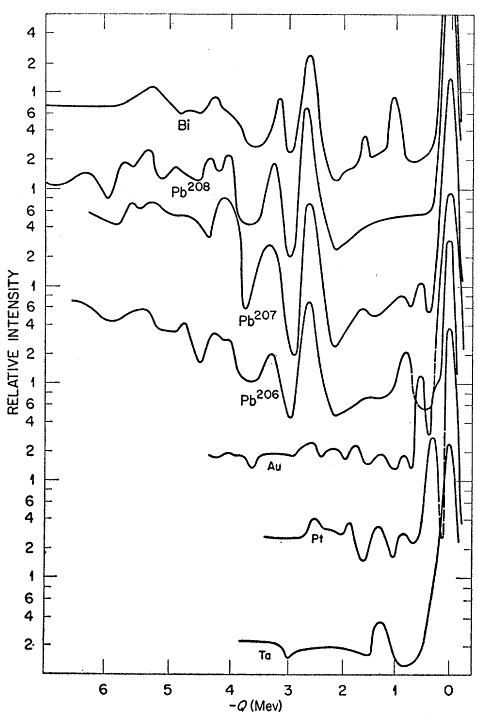


FIG. 8. Energy distribution of protons inelastically scattered from various elements (atomic numbers 73–83) as measured with magnetic analysis. Observation angle was 90 degrees.

In all the cases where the first excited states are resolved in Figs. 6–8, the collective nature of these levels is known to be vibrational. It may be noted that the second vibrational states occurring at about twice the energy are also excited in the data of Figs. 6–8 but nearly an order of magnitude less strongly. This is in accordance with theoretical expectations that the two-phonon vibration is more difficult to excite than the single-phonon vibration. It is furthermore convincing evidence that the anomalous peaks are not higher members of known collective bands.

The low-lying levels of $Pb^{206}$ and $Pb^{207}$ which are shown in Fig. 8 are of special interest because they are also excited in $(p,d)$, $(d,p)$, and $(d,t)$[9] reactions.[2] In comparing the strength with which given levels are excited by $(p,p')$ and the other reactions, there is found to be an anticorrelation. The levels at 0.6, 0.9, and 2.0-Mev excitation in $Pb^{207}$, and the levels at 1.3 and 1.6-Mev excitation in $Pb^{206}$ which are very strongly excited in $(p,d)$, $(d,p)$, and $(d,t)$ reactions are very weakly excited in the $(p,p')$ spectra of Fig. 8, whereas the levels at 2.6-Mev excitation in each of these isotopes are very strongly excited in $(p,p')$ reactions but are apparently not excited appreciably in $(p,d)$, $(d,p)$, and $(d,t)$ reactions. There is very strong theoretical evidence that $(p,d)$, $(d,p)$, and $(d,t)$ reactions excite single-particle levels and recently, new experimental evidence for this has been obtained.[10] The anticorrelation in strengths with which $(p,d)$, $(d,p)$, $(d,t)$, and $(p,p')$

[7] Alder, Bohr, Huus, Mottelson, and Winther, Revs. Modern Phys. **28**, 432 (1956).

[8] A. Bohr, Amsterdam Conference on Nuclear Reaction, July, 1956; Physica **22**, 963 (1956).

[9] J. A. Harvey, Can. J. Phys. **31**, 278 (1953).

[10] B. L. Cohen and A. G. Rubin (to be published).

TABLE I. $Q$ values for peaks (Mev).

| 90° | 45° | Known |
|---|---|---|
| | ${}_{26}$Fe | |
| 0.86 | | 0.85 |
| 1.42 | | 1.41 |
| 2.00 | | 2.08 |
| 2.58 | | 2.60 |
| 3.03 | | 2.95 |
| 3.31 | | 3.32 |
| 3.95 | | |
| 4.2 | | |
| 4.5 | | |
| 4.8 | | |
| 5.9 | | |
| 6.2 | | |
| | ${}_{27}Co^{59}$ | |
| 0.41 | | |
| 1.17 | | 1.19 |
| 1.45 | | 1.45 |
| 2.83 | | |
| 3.18 | | |
| 3.62 | | |
| 3.9 | | |
| 4.1 | | |
| 4.6 | | |
| | ${}_{28}$Ni | |
| 1.51 | | 1.45 |
| 2.50 | | 2.51 |
| 3.20 | | |
| | ${}_{29}$Cu | |
| 0.70 | | 0.67 |
| 1.01 | | 1.03 |
| 1.38 | | 1.42 |
| 1.97 | | 1.90 |
| 2.51 | | 2.60 |
| 3.26 | | |
| 3.72 | | |
| | ${}_{30}Zn^{64}$ | |
| 1.02 | | 1.00 |
| 1.83 | | |
| 2.13 | | 2.27 |
| 3.00 | | |
| | ${}_{30}Zn^{68}$ | |
| 1.07 | | 1.10 |
| 1.98 | | 1.91 |
| 2.34 | | |

| 90° | 45° | Known |
|---|---|---|
| | ${}_{30}Zn^{68}$ | |
| 2.68 | | |
| 3.47 | | |
| 3.8 | | |
| 4.1 | | |
| 4.5 | | |
| 4.9 | | |
| 5.1 | | |
| 5.4 | | |
| | ${}_{30}$Zn | |
| | 1.87 | 1.91 |
| | 2.30 | 2.27 |
| | 2.73 | |
| | 2.96 | |
| | 4.32 | |
| | ${}_{31}$Ga | |
| | 2.20 | |
| | 2.55 | |
| | 3.16 | |
| | ${}_{32}$Ge | |
| | 2.53 | 2.49 |
| | 3.04 | 3.04 |
| | 3.26 | 3.32 |
| | 3.82 | |
| | ${}_{33}$As | |
| | 1.77 | |
| | 2.29 | |
| | 2.57 | |
| | ${}_{34}$Se | |
| 0.24 | | |
| 0.68 | | 0.64 |
| 0.99 | | |
| 1.39 | 1.40 | 1.31 |
| 1.70 | 1.71 | |
| 2.08 | 2.08 | 1.98 |
| 2.47 | | 2.39 |
| 2.63 | 2.61 | |
| 2.88 | | |
| 3.16 | 3.16 | |
| | ${}_{36}$Kr | |
| 0.93 | | 0.89 |
| 2.63 | | 2.7 |
| 2.97 | | |

| 90° | 45° | Known |
|---|---|---|
| | ${}_{37}$Rb | |
| | 2.25 | |
| | 2.50 | |
| | ${}_{38}$Sr | |
| | 1.94 | 1.85 |
| | 2.57 | |
| | 2.77 | 2.76 |
| | 3.56 | 3.52 |
| | ${}_{39}$Y | |
| | 1.86 | |
| | 2.27 | |
| | 2.58 | |
| | 2.91 | |
| | 3.86 | |
| | ${}_{40}$Zr | |
| 0.92 | | 0.93 |
| 1.45 | 1.47 | |
| 2.07 | 2.09 | |
| 2.24 | 2.27 | 2.30 |
| 2.70 | 2.69 | |
| 3.00 | | |
| | ${}_{41}$Nb | |
| 0.74 | | 0.76 |
| 0.94 | 0.95 | 0.98 |
| 1.32 | 1.47 | |
| 1.58 | 1.79 | |
| 2.12 | 2.27 | |
| 2.52 | | |
| 2.77 | 2.92 | |
| 3.05 | | |
| | ${}_{42}$Mo | |
| | 1.04 | |
| | 1.59 | |
| | 2.34 | |
| | 2.61 | |
| | 2.88 | 2.73 |
| | ${}_{45}$Rh | |
| 0.34 | | 0.34 |
| 0.87 | | |
| 1.32 | | |
| 2.04 | | |

| 90° | 45° | Known |
|---|---|---|
| | ${}_{46}$Pd | |
| 0.45 | 0.58 | 0.47 |
| 1.09 | 1.21 | 1.13 |
| 2.11 | 2.28 | |
| 2.75 | 2.81 | |
| | ${}_{47}$Ag | |
| 0.39 | | 0.36 |
| 0.94 | | |
| 1.50 | | |
| 2.19 | | |
| | ${}_{48}Cd^{113}$ | |
| 0.58 | | 0.62 |
| 1.40 | | |
| 2.91 | | |
| | ${}_{48}Cd^{114}$ | |
| 0.58 | | 0.56 |
| 1.30 | | 1.29 |
| 1.92 | | 1.86 |
| 2.33 | | |
| 3.19 | | |
| | ${}_{49}$In | |
| 0.63 | | 0.56 |
| 1.14 | | 1.14 |
| 1.48 | | |
| 2.15 | | |
| 2.43 | | |
| 3.07 | | |
| | ${}_{50}$Sn | |
| 1.18 | 1.39 | 1.20 |
| 2.32 | 2.48 | |
| 3.26 | 3.20 | |
| | 3.54 | |
| | ${}_{52}$Te | |
| 0.79 | 0.83 | 0.78 |
| 1.41 | | 1.38 |
| 2.35 | 2.23 | |
| | 2.54 | |
| | 2.86 | |
| 3.05 | 3.11 | |
| | ${}_{55}Cs_{53}$I | |
| 0.74 | | 0.75 |
| 1.30 | | |

| 90° | 45° | Known |
|---|---|---|
| | ${}_{55}Cs_{53}$I | |
| 1.94 | | |
| 2.32 | | |
| | ${}_{73}Ta^{181}$ | |
| 1.34 | | |
| | ${}_{78}$Pt | |
| 0.34 | | |
| 0.92 | | |
| 1.46 | | |
| 1.99 | | |
| 2.61 | | |
| | ${}_{79}Au^{197}$ | |
| 0.28 | | 0.27 |
| 0.59 | | 0.55 |
| 0.92 | | |
| 1.37 | | |
| 1.84 | | |
| 2.28 | | |
| 2.70 | | |
| | ${}_{82}Pb^{206}$ | |
| 0.87 | | 0.80 |
| | 2.65 | |
| | 3.99 | |
| | ${}_{82}Pb^{207}$ | |
| 0.62 | | 0.57 |
| 0.94 | | 0.89 |
| 1.67 | | 1.63 |
| | 1.81 | |
| | 2.32 | 2.35 |
| | 2.74 | 2.71 |
| | 3.20 | |
| | 3.99 | |
| | 4.24 | 4.27 |
| | 4.58 | 4.62 |
| | 5.14 | 5.20 |
| | ${}_{82}Pb^{208}$ | |
| | 2.66 | 2.62 |
| | 3.18 | |
| | ${}_{83}Bi^{209}$ | |
| 0.88 | | 0.90 |
| 2.66 | | 2.60 |
| 3.16 | | |

reactions excite given levels therefore suggests that $(p,p')$ reactions do not induce single-particle transitions, and that levels strongly excited by these reactions are probably collective. This is the same conclusion as was obtained above from the correlation with Coulomb excitation data.

Another application of the data of Figs. 6–8 is to nuclear spectroscopy. Many of the peaks in these figures correspond to levels not previously reported. The energies of these peaks are listed in Table I. These are probably not single levels in many cases. The spectra of Ge and Se, and of As and Rb are strikingly similar, perhaps indicating that the levels of the major isotopes have a common shell-model origin.

In addition to the general surveys of Figs. 6–8, three cases of isotopic effects were studied. Since the phenomenon of anomalous inelastic scattering seems to start with zinc [1] it is interesting to see whether the effect is present in all isotopes of zinc. Measurements were therefore, made with isotopically separated $Zn^{64}$ and $Zn^{68}$; the results along with those for natural zinc, are shown in Fig. 10. The anomalous peak occurs in both isotopes, but the energy is shifted by about 0.2 Mev. In fact the double peak in natural zinc appears to be due to this isotopic shift.

Up to this point, no nucleus with an odd number of neutrons had been investigated. To fill this gap measurements were made for $Cd^{113}$ and $Cd^{114}$, the former being an odd-neutron nucleus. The results are also shown in Fig. 10. The anomalous peak is present in both isotopes with approximately equal strength but here again the similarity is only in the gross structure; the fine structures of the two curves are quite different.

The case of $Cd^{114}$ is especially interesting, since one of the levels contributing very strongly to the anomalous peak is a known level with known spin and parity. It is listed in Table II, which is a compilation of such data.

The nucleus $Zr^{90}$ is interesting since it contains a magic number of neutrons (50) and a semimagic number of protons (40), and its level structure is well known. Unfortunately, the separated isotope could not be obtained as a metal foil; it was necessary to use a target of the oxide suspended in polystyrene. The results for this target and for natural zirconium are included in Fig. 11.

Some of the data obtained in the third experiment (extension to previously unstudied elements) is also of interest from the high resolution standpoint. These data are shown in Fig. 11; here again, it is evident that the similarities among neighboring elements do not extend to the fine structure. In addition, two more levels of known spin and parity are resolved; namely, the 1.8- and 2.7-Mev levels in $Sr^{88}$. They are listed in Table II. The energies at which various peaks occur are listed in Table I along with similar data for Figs. 6–8.

### 3. Extension to Previously Unstudied Elements

Since the similarities among neighboring elements are more difficult to observe in high-resolution data, the data of Fig. 11 are shown in Fig. 12 smeared out to 0.45-Mev resolution. From that figure, it is clearly evident that the anomalous peak continues uninterrupted from $_{30}Zn$ to $_{40}Zr$. The only exception is Sr whose

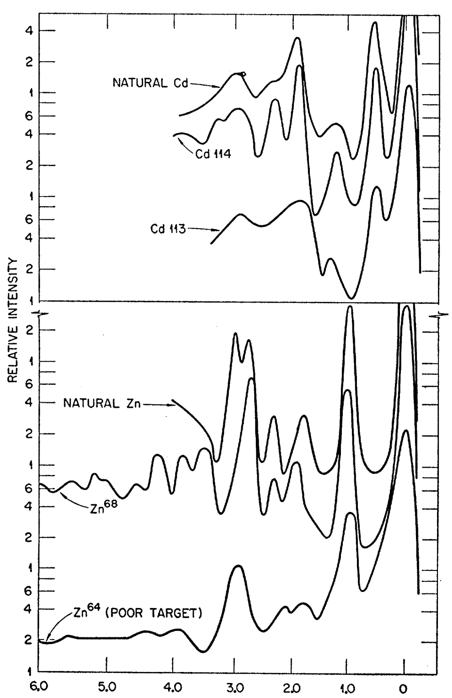


FIG. 10. Energy distributions of protons inelastically scattered from some separated isotopes compared with those from natural elements. Observation angle was 90 degrees.

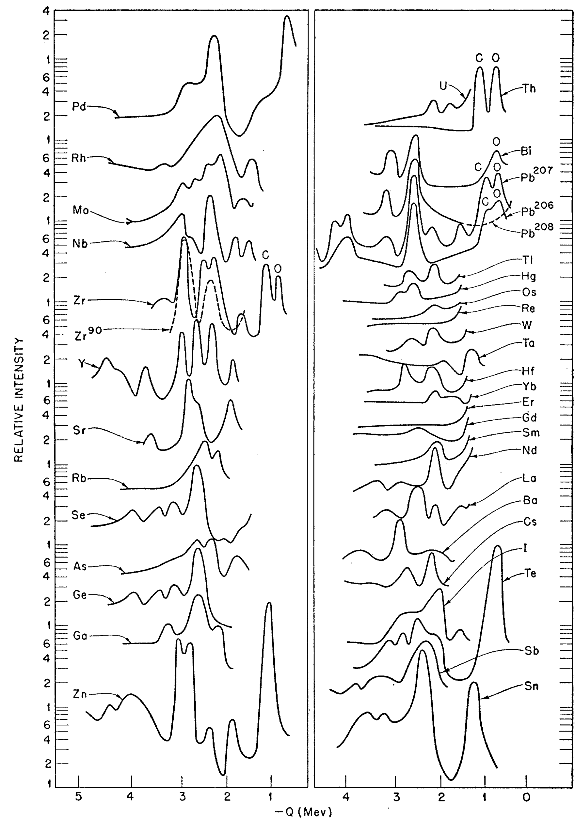


FIG. 11. Energy distributions of protons inelastically scattered from various elements. Many of the targets were very nonuniform and contained large amounts of carbon and oxygen. Observation angle was 45 degrees.

principle isotope contains a closed shell of 50 neutrons and apparently has no levels available in the anomalous region. However, the levels closest to it on each side are strongly excited. It is also interesting to note the rapid shift in the energy just above zinc. In fact, there is a considerable shift among the isotopes of zinc itself, as shown in Fig. 10.

In the region between $_{52}Te$ and $_{78}Pt$, many strange things occur. Between $_{53}I$ and $_{64}Gd$, the anomalous peak seems to be present, but its energy shifts somewhat from element to element. Part, but not all, of this may be due to the closed shell at 82 neutrons. Beyond Gd, where nuclei become permanently distorted, the anomalous peak seems to be weak or absent. Thus, the anomalous peak seems to end gradually as a function of atomic

TABLE II. Spins and parities of known levels in anomalous peak.

| Isotope | $-Q$ (Mev) | $S-\pi$ |
|---|---|---|
| $Sr^{88}$ | 1.9 | 2+ |
| $Sr^{88}$ | 2.7 | 3− |
| $Zr^{90}$ | 2.3 | 2+ |
| $Zr^{90}$ | 2.7 | 3− |
| $Cd^{114}$ | 1.9 | 2+ or 4+ |
| $Pb^{208}$ | 2.6 | 3− |

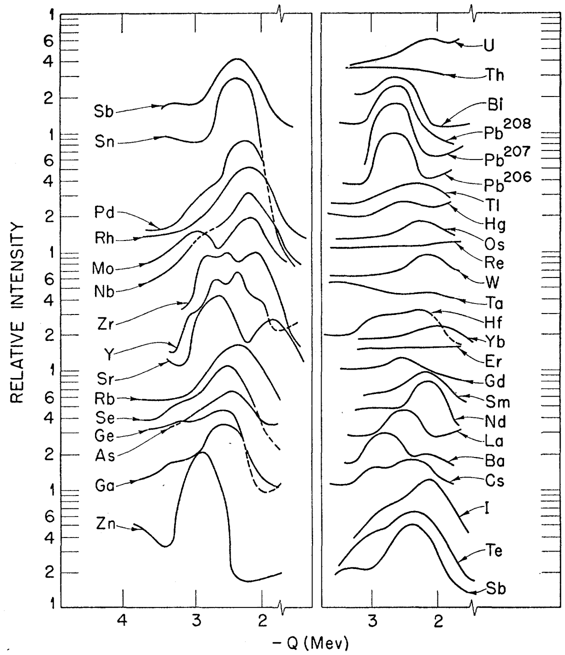


FIG. 12. Data of Fig. 11 with resolution "smeared out" to 0.45 Mev.

number by weakening and becoming irregular in the region between I and Gd; it is interesting to note that this is a region where nuclei are known to become "soft," i.e., deformable with little addition of energy.[11]

From $_{64}$Gd to $_{82}$Pb, there seems to be little regularity. Some elements have anomalous peaks, and some do not. Within each of these groups, there are some even and some odd elements. While there are some cases of striking regularities (e.g., $_{72}$Hf and $_{74}$W), no simple rules seem to govern the situation.

## 4. De-Excitation Gamma Rays

Figure 13 shows some pulse-height distributions in the gamma-ray detector of pulses in coincidence with the anomalous proton peak. A magnesium target was measured for calibration purposes, with the proton detection system set to accept the group at $-Q=4.1$ Mev. This state decays almost exclusively by a cascade of a 2.76-Mev and a 1.38-Mev gamma ray, so that the relative intensities of the two gamma rays are equal, and their probability of occurrence in coincidence with the proton is unity. From the curve for magnesium in Fig. 13, it is clear that the principal peak for any gamma ray up to at least 3-Mev energy is at the full energy. In addition, the efficiencies for gamma rays of 1.38 and 2.76 Mev to give pulses in the full energy peak are determined. This efficiency curve was assumed to be linear with energy for interpolation and extrapolation purposes.

[11] R. K. Sheline, Pittsburgh Conference on Nuclear Structure, June, 1957 (unpublished).

By use of this efficiency determination, the spectrum for silver in Fig. 13 may be shown to be consistent with the assumption that about 50% of all protons in the anomalous peak are followed by a single gamma-ray transition direct to the ground state. On the other hand, it would be difficult to rule out the possibility that the high-energy transitions are preceded by very low-energy (~0.2-Mev) ones, although this would seem to be unlikely. There are some indications of peaks at ~2.4 and 3.3 Mev; these were each reproduced in most runs. They may represent strong proton groups that are not resolved in Fig. 6. The strongest single gamma ray in the spectrum is at 1.8 Mev; it accompanies about 50% of the protons. It may be due to transitions from the peak of the proton spectrum (2.2 Mev) to the first and second excited states (0.32 and 0.42 Mev) of silver.

The gamma-ray spectrum from zirconium shown in Fig. 13 is featured by a strong gamma ray of about 2.2 Mev and a much weaker one at 2.8 Mev. Since these energies are just those of the principal components of the anomalous peak, at least the 2.8-Mev gamma ray must represent direct transitions to the ground state; it follows about 10% of all proton reactions with $-Q\simeq2.8$ Mev. The 2.2-Mev gamma ray occurs in coincidence with a large fraction of all protons in the anomalous peak. A considerable fraction of it must represent transitions to the ground state following proton reactions with $Q=-2.2$ Mev.

If the gamma-ray spectrum from natural zirconium is assumed to be essentially the same as that from its principal isotope, $Zr^{90}$, an interesting conclusion may be drawn from the presence of the strong 2.2-Mev gamma ray. $Zr^{90}$ has two states at about this energy, but one of them has a half-life much longer than the 0.1-microsecond resolving time of the coincidence analyzer so that it would not be observed in coincidence with the proton.

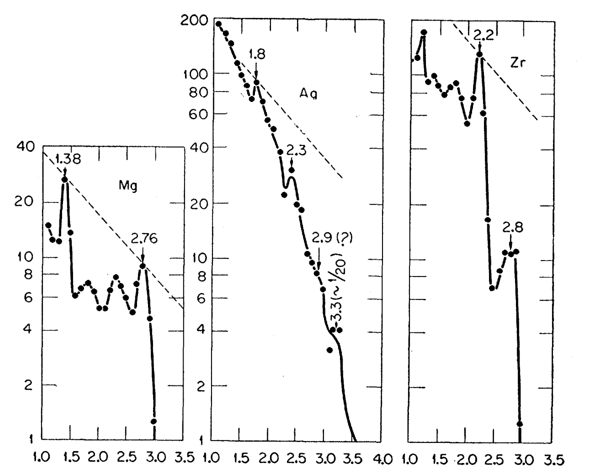


FIG. 13. Pulse-height distribution in gamma-ray detector crystal [3-in. by 3-in. NaI(Tl)] in coincidence with anomalous inelastic scattering from Ag and Zr and with proton peak at $Q=-4.1$ Mev from $Mg(p,p')$.

The state excited is, therefore, the one with a short life time. Its spin and parity are listed in Table II.

## SUMMARY AND DISCUSSION

Some of the principal conclusions that have been drawn in this paper are as follows:

1. Anomalous inelastic scattering is not a giant resonance effect; it is, therefore, undoubtedly due to excitation of some particular type of levels in the final nuclei.

2. The similarities among neighboring elements in the periodic table do not extend to the fine structure. The fine structure exhibits shell effects and odd *vs* even effects, but when the resolution is smeared out these differences disappear, and the energy spectra from neighboring elements—and from different isotopes of the same element—are very similar in the region of the anomalous peak. This indicates that the property which causes these levels to be strongly excited is "dissolved" among many shell-model levels.

3. Both the correlation with Coulomb excitation cross sections and the anticorrelation with $(p,d)$ cross sections for exciting given levels are very convincing evidence that the process involved here—inelastic proton scattering by direct excitation—strongly excites known collective levels and, at least among low-lying levels, does not strongly excite single-particle shell-model levels. This suggests that the anomalous peak, which is due to strongly excited levels, is probably due to a collective mode of excitation, and that it is very probably not due to single-particle excitations.

4. The anomalous peak appears in each of the twenty-one natural elements and in each of the five separated isotopes studied between atomic number 30 and 53. It seems to begin at atomic number 30, and it ends by becoming irregular and weak in the region between atomic numbers 54 and 64. The latter is where nuclei are known to become "soft" and, eventually distorted. As to the former, there is no known discontinuity in nuclear structure involved. One other nuclear phenomenon that does change drastically between atomic numbers 29 and 30 is the ratio of neutrons to protons emitted in nuclear reactions[12]; however, any possible connection between this and anomalous inelastic scattering is not clear. It is also possible that the conclusion about the anomalous peak beginning sharply at atomic number 30 is a misinterpretation of the data.

5. A reasonable number of spins and parities for levels whose excitation lead to the anomalous peak have been accumulated (see Table II). There is some evidence that the lower-energy part of the anomalous peak is due to excitation of positive-parity states, and the higher-energy part is due to negative-parity states. Since both known cases of the latter are $3-$,[13] they can be explained as due to collective octupole oscillations.[14] This would not explain the lower-energy part which includes most of the cross section.[1]

6. The high probability for the states excited in anomalous inelastic scattering to de-excite by gamma-ray emission direct to the ground state excludes the possibility that the effect is due to a volume "breathing mode" as has been suggested[15]; such modes could make only electric monopole transitions to the ground state. This theoretical explanation is also excluded by the spin and parity assignments of Table II since for this type of oscillation in even-even nuclei, the state would be $0+$. The fact that the levels listed in Table II are not $0+$ also makes the theoretical explanation of Tomasini[16] untenable.

## ACKNOWLEDGMENTS

The authors would like to acknowledge the assistance of F. DiCarlo in the data-taking, of E. D. Hudson and R. S. Lord in the magnet modifications, of M. B. Marshall, C. L. Viar, and M. H. Shelton in the cyclotron operation, and the support and encouragement of R. S. Livingston and A. M. Weinberg.

---

[12] B. L. Cohen and E. Newman, Phys. Rev. **99**, 718 (1955).
[13] A state at 2.7 Mev in $Zr^{90}$, which is probably $3-$, has been reported by R. Day (private communication from A. M. Lane).
[14] A. M. Lane and E. P. Pendlebury (private communication); this was also suggested independently by C. Levinson.
[15] W. Heckrotte and J. Uretsky (private communication).
[16] Tomasini, Nuovo cimento **6**, 927 (1957).